the FEBS Journal

Cleavage site analysis of a serralysin-like protease, PrtA, from an insect pathogen *Photorhabdus luminescens* and development of a highly sensitive and specific substrate

Judit Marokházi[1], Nikolett Mihala[2], Ferenc Hudecz[2,3], András Fodor[1], László Gráf[1,4] and István Venekei[1]

1 Department of Biochemistry, Eötvös Loránd University, Budapest, Hungary
2 Department of Organic Chemistry, Eötvös Loránd University, Budapest, Hungary
3 Research Group of Peptide Chemistry, Hungarian Academy of Sciences, Budapest, Hungary
4 Biotechnology Research Group, Hungarian Academy of Sciences, Budapest, Hungary

Keywords
cleavage site; serralysin; specific substrate; metalloprotease; PrtA of *Photorhabdus*

Correspondence
I. Venekei, Department of Biochemistry, Eötvös Loránd University, Budapest, Pázmány Péter sétány, 1/C., 1117, Hungary
Fax: +36 1 381 2172
Tel: +36 1 209 0555/8777
E-mail: venekei@cerberus.elte.hu

(Received 5 December 2006, revised 9 February 2007, accepted 12 February 2007)

doi:10.1111/j.1742-4658.2007.05739.x

The aim of this study was the development of a sensitive and specific substrate for protease A (PrtA), a serralysin-like metzincin from the entomopathogenic microorganism, *Photorhabdus*. First, cleavage of three biological peptides, the A and B chains of insulin and β-lipotropin, and of 15 synthetic peptides, was investigated. In the biological peptides, a preference for the hydrophobic residues Ala, Leu and Val was observed at three substrate positions, P2, P1′ and P2′. At these positions in the synthetic peptides the preferred residues were Val, Ala and Val, respectively. They contributed to the efficiency of hydrolysis in the order P1′ > P2 > P2′. Six amino acids of the synthetic peptides were sufficient to reach the maximum rate of hydrolysis, in accordance with the ability of PrtA to cleave three amino acids from both the N- and the C-terminus of some fragments of biological peptides. Using the best synthetic peptide, a fluorescence-quenched substrate, *N*-(4-[4′(dimethylamino)phenylazo]benzoyl–EVYAVES–5-[(2-aminoethyl)amino]naphthalene-1-sulfonic acid, was prepared. The $\sim 4 \times 10^6$ $M^{-1} \cdot s^{-1}$ specificity constant of PrtA (at $K_m \sim 5 \times 10^{-5}$ M and $k_{cat} \sim 2 \times 10^2$ s^{-1}) on this substrate was the highest activity for a serralysin-type enzyme, allowing precise measurement of the effects of several inhibitors and pH on PrtA activity. These showed the characteristics of a metalloenzyme and a wide range of optimum pH, similar to other serralysins. PrtA activity could be measured in biological samples (*Photorhabdus*-infected insect larvae) without interference from other enzymes, which indicates that substrate selectivity is high towards PrtA. The substrate sensitivity allowed early (14 h post infection) detection of PrtA, which might indicate PrtA's participation in the establishment of infection and not only, as it has been supposed, in bioconversion.

Of the various enzymes that microorganisms secrete for defence as well as for invasion and bioconversion of their environment, proteases have the most diverse functions. Exploration of the enzymatic properties and functions of these proteases may contribute to a better understanding of the pathomechanism and gaining control over the infection process. Few such proteases have been characterized enzymatically and even less is known about their role in the pathomechanism.

Abbreviations
Dabcyl, *N*-(4-[4′(dimethylamino)phenylazo]benzoyl; Dabcyl-OSu, *N*-(4-[4′(dimethylamino)phenylazo]benzoyloxy)succinimide; Edans, 5-[(2-aminoethyl)amino]naphthalene-1-sulfonic acid; OpdA, oligopeptidase A; Php-C, *Photorhabdus* protease C; PrtA, protease A.

The roles played by secreted proteases of two entomopathogenic bacterium groups, *Photorhabdus* and *Xenorhabdus*, might be of special interest because: (a) *Photorhabdus* and *Xenorhabdus* strains are highly pathogenic, and may serve as an excellent pathogen component for an infection model; (b) in nature, survival of these bacteria is strictly dependent on their symbiosis with entomopathogenic nematodes from the families Heterorhabditidae and Steinernematidae, respectively; and (c) bacterium–nematode complexes might be exploited in environmentally friendly insect biological control technologies. Secretion of three proteases has been detected in *Photorhabdus* [1], which is better characterized at the molecular level than *Xenorhabdus*. Two of these, *Photorhabdus* protease C (Php-C) and protease A (PrtA), were identified by their sequences [1–3]; Php-C is a metallopeptidase from the M4 (thermolysin) family, whereas PrtA (first found in *Erwinia chrysantemi*), belongs to the 50 kDa bacterial metallo-endopeptidases, the serralysins, a subfamily of the interstitial collagenase family (M10). The intensively studied proteases in the latter subfamily, beside the ~56 kDa metallo-endoprotease of *Serratia marcescens* (serralysin), are the alkaline proteinase of *Pseudomonas aeruginosa*, the ZapA metalloprotease of *Proteus mirabilis* and proetases A, B, C, G and W of various *Erwinia* strains. One function of these proteases is thought to be as virulence factors. However, their contribution to pathogenesis cannot be properly assessed because of a lack of information about the dynamics of their production during infection and their proteolytic systems [comprising the protease as well as its natural substrate(s) and inhibitor(s)]. Several potential natural substrates have been found for ZapA of *P. mirabilis* and the 56 kDa protease of *S. marcescens* (IgA and IgG proteins, some defenesins, cytoskeletal proteins, complement system components, extracellular matrix molecules) [4–10], but the *in vivo* significance of cleavage of these proteins remains to be established. According to substrate-specificity studies on synthetic peptides, serralysin, ZapA and alkaline proteinase exhibited relaxed side-chain discrimination at substrate positions P3–P3′ [11–15]. (The scissile bond is between the P1 and P1′ sites, Schechter and Berger's notation [16].) Consistent with this finding was the observation that these enzymes cleaved (denatured) oligopeptide substrates of biological origin at numerous sites in various sequence environments [8,12,17]. These properties do not indicate proteases that have specific sets of natural substrates, and make difficult the development of selective and sensitive substrates for measuring enzyme activity during infection. To date, the best synthetic substrates for serralysin-like enzymes are between six and eight amino acids long and contain mostly hydrophobic P2 and P2′ residues [11–13,15]. Although both the relatively small number of peptide sequence variants and their amino acid composition limit the conclusions that can be drawn about side-chain discrimination in these enzymes, some of the kinetic data on these substrates seem interpretable by the structure of the enzymes' active site [18–21]. It is also important to mention that the usability of these substrates was not tested on biological samples.

For an exploration of the proteolytic system of PrtA, and an understanding of its role in the infection process of *Photorhabdus*, we needed a highly sensitive and specific substrate to selectively measure activity in biological samples. Here we describe the development of such a substrate based on analysis of PrtA cleavage site specificity, and kinetic characterization of PrtA activity on the new substrate.

Results and Discussion

Identification of PrtA cleavage sites in biological peptides

To obtain an initial view of the cleavage-site specificity of PrtA, we analysed the sequence of PrtA hydrolysis sites in three biological peptides, insulin A and B chains, and β-lipotropin. We were able to draw two conclusions from the data (Figs 1–3):

(a) Alignment of the cleavage sites (Fig. 3) showed a preference for hydrophobic amino acids at substrate positions P2, P1′ and P2′, a property that is not pronounced in the case of other serralysins of known specificity. A simple probability analysis of amino acid frequencies (not shown) indicated a slightly higher frequency of Leu and Val at position P2′, which is in accordance with the presence of a conserved Leu (Leu3, a position equivalent to P2′) of the known bacterial inhibitors of serralysin-like proteases [20,22–24]. Because an even longer peptide inevitably samples only a small fraction of all the possible sequence combinations around potential cleavage sites (usually spanning between six and eight amino acids) which might, additionally, be biased by the unique frequency of amino acids in the peptide, the predictive power of such cleavage site analysis on (biological) peptides is restricted. Nonetheless, from our results it could be concluded that PrtA cleavage sequences are rich in the aliphatic amino acids Ala, Leu and Val.

(b) From the dynamics of hydrolysis (estimated from the change in the amount of some fragments) (Figs 1A,2A), it was evident that most of the cleavage

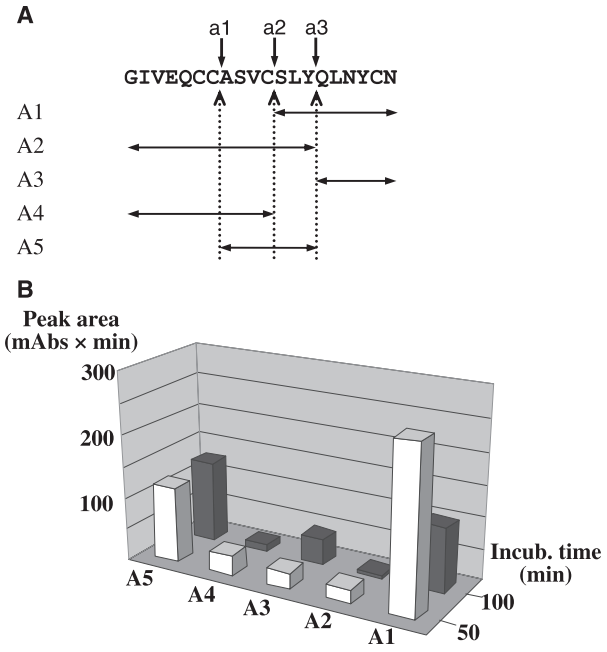

Fig. 1. Cleavage site analysis of PrtA on oxidized insulin chain A. (A) The position of cleavage sites (vertical arrows, a1–a3) and cleavage fragments (horizontal double arrows, A1–A5) in the sequence of insulin chain A. (B) Change over time in the chromatographic peak area of cleavage fragments. Note that the amount of fragments A1, A2 and A4 decreases on longer exposure to PrtA cleavage. (For details see Experimental procedures.)

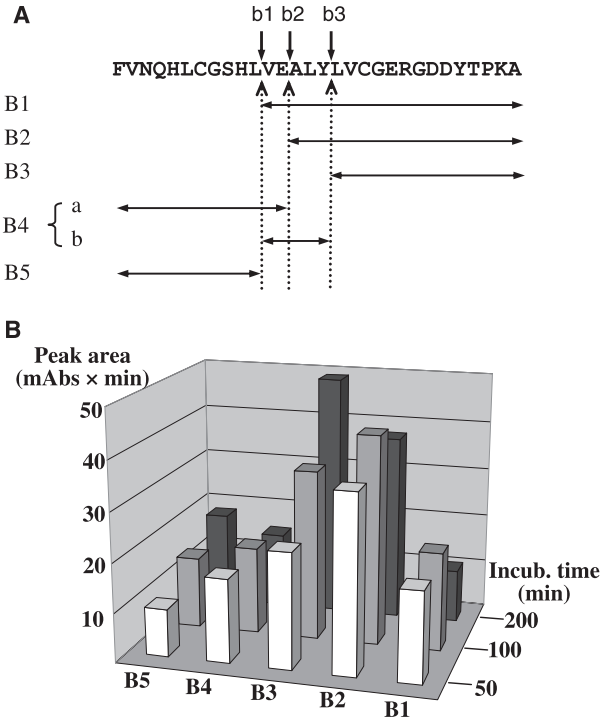

Fig. 2. Cleavage site analysis of PrtA on oxidized insulin chain B. (A) The position of cleavage sites (vertical arrows, b1–b3) and cleavage fragments (horizontal double arrows, B1–B5) in the sequence of insulin chain B. (B) Change over time in the chromatographic peak area of cleavage fragments. Note, that fragments B1, B2 and B4 show a temporary accumulation. Fragments B4a and B4b did not separate under the applied conditions of reverse-phase HPLC. (For details see Experimental procedures.)

sites could serve as sites of secondary cleavage, even if they were only three amino acids from either the C- or the N-terminus. This suggests that PrtA might be able to cleave peptides as short as six amino acids.

Optimization of peptide sequence and length

Supposing that hexapeptides were bound by PrtA such that they span the S3–S3′ enzyme sites in an N- to C-terminal (i.e. P3–P3′) orientation and would be cleaved between amino acids 3 and 4 (peptide positions P1 and P1′, respectively), the amino acids at positions P2, P1′ and P2′ were selected for variation for the following reasons:

(a) They are among the four inner sites (P2–P2′) that contribute most significantly to the proper positioning of the scissile bond in almost every protease.

(b) We found that the side-chain discrimination of PrtA is the most restricted in these positions, with a preference for the aliphatic residues Ala, Leu and Val.

As for the three other positions, we took advantage of the apparent relaxed side-chain preference of PrtA to increase the solubility of the peptides (by choosing Glu at positions P3 and P3′), and Tyr at the (supposed) P1 position, which rendered the peptide segment, N-terminal to the scissile bond, distinguishable at 280 nm. Thus 12 hexapeptides (Pa1–Pa12) were synthesized which contained, in every possible combination, each of the amino acids chosen to vary at positions P2, P1′ and P2′ (Fig. 3).

The results of PrtA hydrolysis of the hexapeptide library are summarized in Table 1 and Fig. 4. For each peptide only two hydrolysis products were observed, showing that they were cleaved at only one bond. With the exception of Pa6 and Pa12 (see Experimental procedures and the legend to Table 1), identification of the cleavage products and determination of the cleaved bond were possible using only the retention times (Table 1). One of the products always absorbed at 280 nm, which identified it as an N-terminal (Tyr-containing) one. There were only two retention times (either 26.2 or 28.8 min), showing that the products were variants of only two sequences. This was possible only if the products differed at position P2, i.e. if the

	P4	P3	P2	P1	P1'	P2'	P3'	P4'
Insulin chain A	E	Q	C	C	A	S	V	C
	A	S	V	C	S	L	Y	Q
	C	S	L	Y	Q	L	N	Y
Insulin chain B	C	G	S	H	L	V	E	A
	H	L	V	E	A	L	Y	L
	E	A	L	Y	L	V	C	G
β-Lipotropin	E	L	A	G	A	P	P	E
	P	A	E	G	A	A	A	R
	L	E	Y	G	L	V	A	E
	S	E	K	S	Q	T	P	L
	P	L	V	T	L	F	K	N
P. luminescens (Inh)				S	S	L	V	L
E. chrysantemi (Inh)				S	S	L	R	L
S. marcescens				G	S	L	A	L
P. aeruginosa				S	S	L	I	L
peptide library (Pa1-12)	Ac	E	{L, V}	Y	{A, L}	{A, L, V}	E	NH_2
the best substrate (Pa4)	Ac	E	V	Y	A	V	E	NH_2

Fig. 3. Alignment of PrtA cleavage sites in three biological peptides and the N-terminal (inhibitory) peptide segment of four inhibitors of serralysin-type enzymes. The sequence variants of the synthetic hexapeptide library (Pa1–Pa12) are also shown aligned in the expected and observed cleavage positions (indicated with a dashed line and a vertical arrow). Inh, is a PrtA inhibitor from *Photorhabdus*.

P1–P1′ peptide bond (on the C-terminal side of Tyr) was cleaved in each case. The same conclusion could be reached for the cleavage of these peptides if the retention times of C-terminal hydrolysis fragments and the possible sequences were coupled.

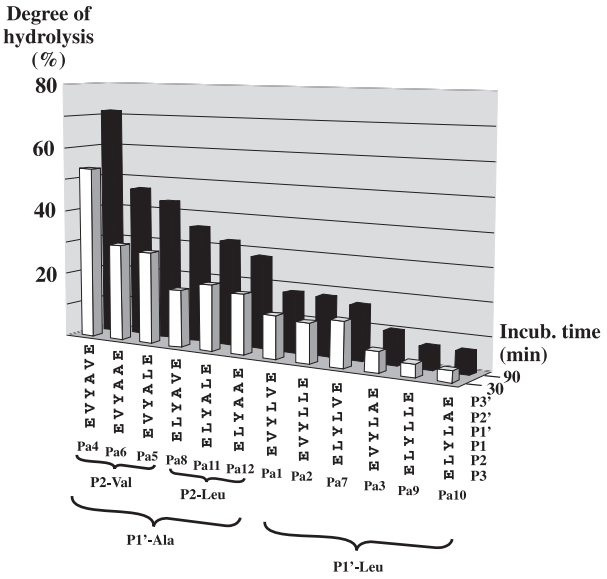

Fig. 4. Variants of the hexapeptide library ranked by the degree of hydrolysis. The ranking is according to the degree of peptide hydrolysis after 90 min incubation at 0.25 mM peptide and 0.36 nM PrtA concentrations. Links indicate groups (P1′ Ala or Leu) and subgroups (P2 Leu or Val). (For further details see Experimental procedures.)

When library peptides were ranked in the order of degree of hydrolysis (Fig. 4), groups and subgroups became evident depending on the amino acid at

Table 1. Reverse-phase HPLC analysis of cleavage of the hexapeptide library. nd, not detectable under the chromatographic conditions used.

		Retention times (min)								
			Products							
			P3–P1		P1′–P3′					
Substrates	Substrate position 3211′2′3′	Peptide	EVY	ELY	LVE	LLE	LAE	ALE	AVE	AAE
Pa1	Ac-EVYLVE-NH_2	32.1	26.2		22.0					
Pa2	Ac-EVYLLE-NH_2	34.6	26.2			25.0				
Pa3	Ac-EVYLAE-NH_2	30.6	26.2				20.2			
Pa4	Ac-EVYAVE-NH_2	28.2	26.2						nd	
Pa5	Ac-EVYALE-NH_2	30.9	26.2					21.0		
Pa6	Ac-EVYAAE-NH_2	25.5[a]	25.1[a]							nd
Pa7	Ac-ELYLVE-NH_2	34.0	28.9		22.0					
Pa8	Ac-ELYAVE-NH_2	30.4		28.9					nd	
Pa9	Ac-ELYLLE-NH_2	36.3	28.9			25.0				
Pa10	Ac-ELYLAE-NH_2	32.3	28.9				20.2			
Pa11	Ac-ELYALE-NH_2	32.8	28.9					21.0		
Pa12	Ac-ELYAAE-NH_2	28.4[a]		28.8[a]						nd

[a] Retention times of hydrolysis fragments of these peptides are not comparable with those of the others because different chromatography conditions had to be applied (see Experimental procedures).

positions P1′ and P2, respectively. This allowed assessment of the contribution the three positions and their amino acids made to hydrolysis efficacy. Also, within the limits of the library sequence set, it provided information about the preferred cleavage site sequence. For example, each of the first six, best cleaved, peptides have Ala at the P1′ site (P1′-Ala group), whereas each of the three best substrates within this group have Val at the P2 site (P2-Val subgroup). Analysis of the data in Fig. 4 suggests that if P1′ is Ala then Val is better than Leu at the P2 position, regardless of the amino acid at position P2′. This preference for Val over Leu at the P2 site can also be seen in the P1′-Leu group, but here, the fact that Val is the best residue at the P2′ site has some influence on the preferred residue at P2 (peptide Pa7 is better than Pa3). Thus, of the three positions varied in our hexaeptide library, the contribution of P1′ to cleavage efficacy is the strongest and that of P2′ is the weakest, with an Ala, Val and Val preference at positions P1′, P2 and P2′, respectively.

Of the 14 residues at sites S1–S3′ that contact the inhibitor in the crystal structure of inhibitor enzyme complexes of serralysin and alkaline protease, only three differ in PrtA: Ser132, Tyr133 and Phe217, but only the latter two appear to be significant. (These are Gln/Ala and Trp, respectively, in other serralysins, serralysin numbering.) Because these positions are involved mainly in formation of the S1′ and S2′ sites [20,25], in PrtA the differences may cause an increase in hydrophobicity and some reshaping at these sites. This may explain the higher preference of PrtA for aliphatic segments in biological peptides, and the preference for Val over Leu at the P2′ substrate position, relative to other serralysins [11–13,15].

Because the best peptide, Pa4, was cleaved almost twice as fast as the second best (Pa6), we chose Pa4 to construct a chromogenic substrate. Keeping its sequence, we made extensions to the C-terminus by the addition of one (Ser or Tyr) or two (Ser–Tyr) amino acids to examine the effect of a longer peptide chain on cleavage. Neither extension influenced the rate of hydrolysis (data not shown) indicating that PrtA is able to cleave three amino acids from the peptide ends, and also that a length of six amino acids is enough for efficient substrate binding and hydrolysis.

It was evident from the peptide hydrolysis that for efficient cleavage PrtA requires interactions with the substrate on both sides of the scissile bond. To allow all such interactions to form, we designed a fluorescence-quenched substrate. Linkage of a quencher and a fluorophore to Pa4 hexapeptide would have been their closest positioning, ensuring the most efficient fluorescence quenching, and thereby the highest possible sensitivity of activity measurement. However, to reduce the possibility of interference of the chromophores with binding of the peptide to the enzyme, which could not be excluded in this case and might have compromised the specificity of the substrate, we conjugated the quencher *N*-(4-[4′(dimethylamino) phenylazo]benzoyl (Dabcyl) and the fluorophore 5-[(2-aminoethyl)amino]naphthalene-1-sulfonic acid (Edans) to one of the extended forms of Pa4 hexapeptide, and prepared the Dabcyl–EVYAVES–Edans substrate. When PrtA hydrolysis of this substrate was followed using HPLC and mass spectrometry (see Experimental procedures), it was found that conjugation of the quencher and the fluorophore influenced neither the rate nor the site of hydrolysis of the peptide.

Sensitivity and selectivity of the Dabcyl–EVYAVES–Edans substrate and the activity of PrtA

After determining the optimal excitation and emission wavelengths, the molar fluorescence value and the calibration of the inner filter effect (see Experimental procedures), the kinetic parameters of four PrtA preparations (the two isoforms, PrtAi and PrtAii, their mixture and the recombinant form of PrtA) were determined along with those of several other enzymes (Table 2). The PrtA preparations exhibited approximately the same, high-specificity constants ($\sim 2.3 \times 10^6$ $M^{-1} \cdot s^{-1}$), which were one order of magnitude higher than the highest constant for a serralysin-like enzyme measured to date (ZapA of *P. mirabilis*) [14], and 100-fold higher than the specificity constants

Table 2. Kinetic parameters of PrtA and comparison of the specific activity of PrtA to several other enzymes on Dabcyl–EVYAVES–Edans substrate.

	k_{cat} ($\times 10^2$ s^{-1})	K_M ($\times 10^{-5}$ M)	k_{cat}/K_M ($\times 10^6$ $s^{-1} \cdot M^{-1}$)	Substrate specificity[a]
PrtA[b]	2.10 ± 0.3	9.0 ± 0.2	2.34	1.00
PrtAi	1.67 ± 0.3	7.0 ± 0.3	2.39	–
PrtAii	1.27 ± 0.2	5.0 ± 0.1	2.54	–
Recombinant PrtA	2.30 ± 0.6	11.0 ± 4.0	2.09	–
OpdA			0.023	~ 0.01
Php-C			0.024	~ 0.01
Clostridium collagenase			0.0044	~ 0.002
Trypsin			0.0056	~ 0.0024
Chymotrypsin			0.026	~ 0.01

[a] The specificity of the substrate was calculated as the ratio of specific activities of the different enzymes relative to PrtA. [b] A PrtA preparation containing both PrtAi and PrtAii variants.

of matrixins, the enzymes in the other subfamily of interstitial collagenases, on their synthetic substrates [26]. Relative to the parameters of ZapA on its best substrate, the Michaelis constant (K_m) and the catalytic efficiency (k_{cat}) values for PrtA on our substrate were 2- and 100-fold higher, respectively, suggesting weaker ground-state stabilization and better positioning of the scissile bond. Comparable activities of metallo-peptidases on synthetic substrates have been reported for *Clostridium hystolyticum* collagenase (M26 family) [27] and peptidases in the thimet oligopeptidase (M3) family [28,29]. The Dabcyl–EVYAVES–Edans substrate allowed detection of as low as 1–3 pmoles of enzyme at a substrate concentration of 55 μM, which is a 3–10-fold higher sensitivity of detection for PrtA activity than achieved with zymography (10–20 pmoles; not shown). (Using a higher substrate concentration, closer to saturation, would not increase sensitivity further. Moreover it would decrease sensitivity because of the stronger inner filter effect.) The selectivity of the substrate for PrtA (comparison of k_{cat}/K_m values) proved at least two orders of magnitude larger than for other proteases (Table 2), *Clostridium* collagenase (clostridial collagenase family, M31), Php-C (thermolysin family, M4) and oligopeptidase A (OpdA; thimet oligopeptidase family, M3), as well as trypsin and chymotrypsin (chymotrypsin family of serine proteases, S1).

Because the high sensitivity and specificity of our substrate gave, for the first time, the opportunity for precise PrtA activity measurements, we investigated the effects of several inhibitors and pH on *Photorhabdus* PrtA. The enzyme could be inhibited by metal ion chelators (EDTA and 1,10-phenantroline, as reported previously) [2,30,31], but not by a reagent of active serine (phenylmethanesulfonyl fluoride), while disulfide bridge-reducing agents (1,4-dithiothreitol and Cys) and SH group reagents (Cys) were inhibitory to different degrees (Table 3), although there is no cystein in the sequence of PrtA. Inhibition by these compounds could be rescued by the presence of 1.5 mM Zn^{2+} during activity measurement, indicating a reversible effect for 1,4-dithiothreitol and Cys on the function of the catalytic Zn^{2+}. However, this was probably not the removal of the ion but, perhaps, was due to a binding to the catalytic metal ion [25,32]. By contrast, the two strong chelators had an irreversible effect. A similar loss of PrtA activity during incubation with EDTA was reported by Bowen *et al.* [2] and was found to be due to destabilization of the structure against autolysis.

Table 3. The effect of several inhibitors on PrtA activity. ND, not determined. For the pretreatment of PrtA with the inhibitors, 0.4 nM enzyme was incubated for 20 min in the presence of 1.0 mM inhibitor. The remaining activity was measured in both the absence (–) and presence (+) of added Zn^{2+} (to 1.5 mM final concentration) as the initial velocity of the reaction which was started by the addition of 1.0 μM substrate. The remaining activities are expressed as per cent control (enzyme incubation without inhibitor, activity measurement without the presence of Zn^{2+}).

	Remaining activity (% of control)	
1.5 mM Zn^{2+} addition: inhibitor (1.0 mM)	–	+
–	100	86
phenylmethanesulfonyl fluoride	95	ND
EDTA	5.5	21
1,10 phenantroline	12	16
1,4-dithiothreitol	15	100
cysteine	68	88

The pH profile for PrtA activity showed a broad pH optimum (6–9) and two peaks (around pH 6.5 and 8.5) (Fig. 5), similar to serralysin and alkaline proteinase

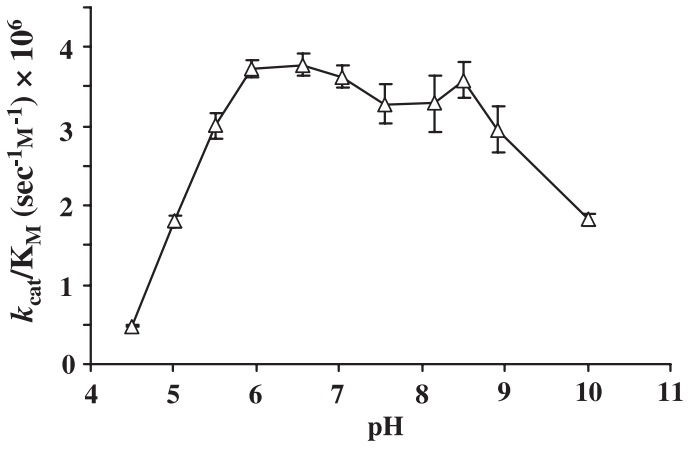

Fig. 5. pH profile of PrtA activity. The k_{cat}/K_m values are calculated from initial reaction velocities (see Experimental procedures) at 1.0 μM Dabcyl–EVYAVES–Edans substrate and 0.2 nM enzyme concentrations. Each point is the average of three measurements.

[33]. Precise determination of the pK values for PrtA was not possible at the resolution of pH scale in our measurement.

PrtA activity in biological samples from *Photorhabdus*-infected insects

In order to test whether the selectivity and sensitivity of the substrate are sufficient for measurements in biological samples, we investigated the dynamics of PrtA production, which is important for understanding the physiological role(s) of PrtA. To date, the activity of this enzyme in biological samples has been assayed only by the semi-quantitative method of zymography, using nonspecific substrates, casein and gelatin [1,2,34]. Our Dabcyl–EVYAVES–Edans substrate could not be used for PrtA activity measurement in *Photorhabdus* culture supernatant because of very high background fluorescence in the culture medium. However, it was excellent in the case of samples from *Photorhabdus*-infected insects because it proved to be very specific for PrtA activity. No enzyme in either the haemolymph or other body compartments produced detectable cleavage at a 1 μM substrate concentration, and at 20 μM, which allowed a fivefold higher sensitivity, the nonspecific activities remained just above the detection limit (5–50 cps·s^{-1} not shown). This selectivity, sensitivity and the quantitative nature of measurements revealed properties of PrtA production that were inaccessible using zymographic detection (Fig. 6):

a) PrtA activity was first detected at ~ 14 h post infection (in the first stage of infection), 6–9 h earlier than in previous detections using zymography, although its level remained highly variable between larvae until the ~ 30 h post infection.

b) At 14 h post infection the activity was mainly in the tissues, as indicated by a sixfold higher activity in the body homogenate than in the haemolymph (494 ± 342 versus 8.8 ± 3.8 cps·s^{-1}). These observations might indicate participation of PrtA in the establishment of infection.

c) The initial low activity increased several hundredfold by around 40 h post infection, at approximately the beginning of the second, symbiotic stage of infection [35] when, among others, an intensive bioconversion of the cadaver starts supporting the assumption that PrtA takes part in the degradation of host tissues. With the exception of several minor components of haemolymph, however, PrtA was not able to cleave the native proteins tested: albumin, fibrinogen and types I and IV collagens (data not shown). A further, interesting possibility to explain the high PrtA activity in the later stage of infection might be that it is needed for the symbiotic interaction between *Photorhabdus* and its nematode partner.

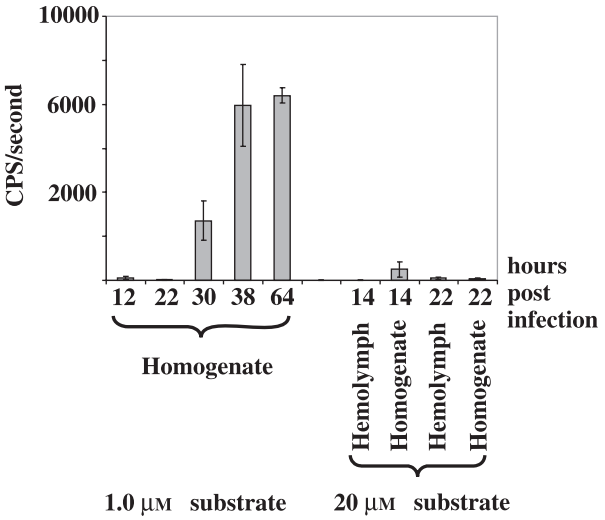

Fig. 6. Measurement of PrtA activity in biological samples from *Photorhabdus*-infected *G. mellonella* larvae. The initial hydrolysis rate was determined in 10–20 μL of 10-fold diluted haemolymph and body homogenate samples (see Experimental procedures) at 1.0 μM and 20 μM Dabcyl–EVYAVES–Edans substrate concentrations, and was calculated for 1.0 μL undiluted sample.

Experimental procedures

Enzymes

Bovine trypsin and chymotrypsin and *Clostridium* collagenase were purchased from Sigma-Aldrich (St. Louis, MO). *Photorhabdus* proteases, PrtA, OpdA and PhpC, were prepared as described previously [1,28].

Biological peptides and the materials of substrate synthesis

Biological peptides, insulin chains A and B and β-lipotropin, were from Sigma. The N^{α}-Fmoc-protected amino acids and the solvents used for the synthesis were purchased from Reanal Fine Chemical Works (Budapest, Hungary). The side-chain-protecting group was *tert*-butylester for Glu and *tert*-butyl for Ser and Tyr. 4-(2′,4′-Dimethoxyphenyl-Fmoc-aminomethyl)phenoxy (Rink amide), 2-chlorotrityl chloride and *N*-(4-[4′(dimethylamino)phenylazo]benzoyloxy)succinimide (Dabcyl-OSu) were from Novabiochem (Laufelfingen, Switzerland). Edans sodium salt was from Invitrogen Molecular Probes (Carlsbad, CA). *N*-Hydroxybenzotriazole, trifluoroacetic acid, 1,8-diazabicyclo[5.4.0]undec-7-ene and *N*,*N*′-diisopropylcarbodiimide were from Fluka (Buchs, Switzerland).

Peptide synthesis

The hexapeptide library and the extended forms were synthesized using a solid-phase technique on an automated multiple-peptide synthesizer (Syro, MultiSynTech, Witten, Germany) using Rink amide resin (30 mg, resin loading 0.45–0.51 mmol·g^{-1}). Peptide chain assembly was performed using Fmoc-strategy and a double-coupling procedure with a fivefold excess of Fmoc-amino acid, *N*-hydroxybenzotriazole, and *N*,*N*′-diisopropylcarbodiimide (1 : 1 : 1 v/v/v) in dimethylformamide (2 × 40 min). The Fmoc-deprotection step was accomplished by 20% 1,8-diazabicyclo[5.4.0] undec-7-ene in dimethylformamide for 3 × 10 min.

The N^{α}-Dabcyl-labelled peptide was synthesized manually on 2-chlorotrityl chloride resin (200 mg, resin loading 0.72 mmol·g^{-1}) using side-chain-protecting groups and the protocol described above. For the N-terminal labelling 3 eq. Dabcyl-OSu was applied. The N^{α}-Dabcyl-labelled and side-chain-protected peptide was removed from the resin with a mixture of dichloromethane/MeOH/acetic acid (80 : 15 : 5 v/v/v). Edans was introduced to the N^{α}-Dabcyl-labelled protected peptide in dimethylformamide using *N*,*N*′-diisopropylcarbodiimide/*N*-hydroxybenzotriazole. The product was isolated by semi-preparative HPLC.

Removal of the protecting groups and, in the case of the library, removal of the amino acid side-chain-protecting groups, and peptide cleavage from the resin were accomplished using the cleavage mixture trifluoroacetic acid/triisopropyl silane/water (95 : 2.5 : 2.5 v/v/v) for 2 h at room temperature. Fully deprotected peptides were precipitated from ice-cold diethyl ether. Suspensions were centrifuged, the ether was decanted, and the peptides were suspended in fresh ether and centrifuged. Washing with cold ether was repeated four times. Finally, the peptides were dissolved in acetic acid and lyophilized.

Crude product was purified by reverse-phase HPLC with 230 nm UV detection on a semi-preparative C_{18} Vydac 218TP 1022 column (Hesperia, CA) eluted at 10 mL·min^{-1} with a 70 min 10–60% linear gradient of 5% acetonitrile/0.025 M ammonium acetate, pH 7 in water (solvent A)/20% 0.025 M ammonium acetate, pH 7 in acetonitrile (solvent B). Peptides were characterized by ESI-MS and analytical reversed-phase HPLC with 214 nm UV detection on a YMC-Pak ODS C_{18}, 120 Å, 5 μm (4.6 × 150 mm) (Schermbeck, Germany) column using 0.1% trifluoroacetic acid in water (A) and 0.08% trifluoroacetic acid in acetonitrile (B) as the eluting system (20–70% B over 35 min at a flow rate of 1 mL·min^{-1}). Molecular masses were measured by ESI-MS, performed on a Bruker Daltonics Esquire 3000 plus (Bremen, Germany) mass spectrometer.

Bacterium strains and culturing

P. luminescens ssp. *laumondii* strain Brecon was from the entomopathogenic nematode/bacterium strain collection maintained at the Department of Genetics, Eötvös Loránd University, Budapest. Single colonies were grown for 48 h on Luria–Bertani plates and were used to start liquid cultures in Luria–Bertani medium, at 30 °C without antibiotics. For the recombinant PrtA preparation *Escherichia coli* XL1 Blue cells were transformed with pUC19 plasmid (New England Biolabs, Beverly, MA) containing the *prtA* operon (kind provided by R. ffrench-Constant, University of Bath, UK), and were grown on Luria–Bertani plates and in Luria–Bertani medium in the presence of 100 μg·mL^{-1} ampicillin.

Experiments with insect larvae

Fourth-instar *Galleria mellonella* (greater wax moth, Lepidoptera) larvae, bred in our laboratory, were infected by injection of 50–100 *P. luminescens*, var. Brecon cells in 5 μL sterile NaCl/P_i. Haemolymph and body homogenate samples, which were cell-free and diluted 10× in 0.25 μg·mL^{-1} phenylthiourea containing NaCl/P_i, were prepared as described earlier [1].

Identification of PrtA cleavage sites in biological peptides

Insulin A and B chains and β-lipotropin were digested with PrtA at 30 °C, in 50 mM Tris/HCl buffer (pH 8.0) containing 10 mM $CaCl_2$ and 0.1 M NaCl, at 1.5 nM enzyme and 0.25 mM substrate concentrations. Reactions were stopped by the addition of 100 μL reaction mixture to 20 μL of 5.0 M acetic acid, and the peptide composition of the samples was analysed by reverse-phase HPLC on a Macherey-Nagel Nucleosil 300–5 C_{18} (100 × 6 × 4 mm) column (Düren, Germany), using a 0–65% linear acetonitrile gradient (2%·min^{-1}) in 0.1% trifluoroacetic acid, at a flow rate of 1.0 mL·min^{-1}. The peptides in the effluent were detected at 220 nm. Elution peaks were collected and lyophilized for determination of fragment mass with a HP Series 1100 mass spectrometer (Agilent Technologies, Santa Clara, CA) in electrospray mode (Gábor Juhász, ELTE-MTA Research Group of Neurochemistry). Mass-based identification of fragment sequence was performed using PAWS software (Harvard Bioscience Inc., Boston, MA).

Hydrolysis of synthetic peptides

Hydrolysis conditions were the same as described for the biological peptides except that the enzyme concentration was 0.36 nM. Samples were prepared by withdrawal of 24-μL aliquots from the reactions and the addition of 5.0 M acetic acid to a final concentration of 1.0 M. These samples were loaded onto a Zorbax 300 SB C_{18} (250 × 4.6 mm) column (Agilent Technologies) and eluted after a 7-min 0% isocratic phase with a 0–40% linear gradient of acetonitrile

(1.6%·min^{-1}) in 0.1% trifluoroacetic acid, at 1.0 mL·min^{-1}. Because under these conditions the intact peptides Pa6 and Pa12 and their hydrolysis products did not separate well, to analyse the hydrolysis of these peptides the above chromatography conditions were modified such that a 2-min 0% isocratic phase was followed by a 0–30%, 0.86%·min^{-1} linear gradient. Elution was monitored at 220 and 280 nm and, in the case of the Dabcyl–EVYAVES–Edans substrate, also at 495 nm, where the Dabcyl quencher group absorbs. For comparison of hydrolysis rates, 0.25 mM furylacryloyl-LGPA was added to the hydrolysis reactions as an internal standard, because it was not hydrolysed by PrtA. Peak areas were normalized with the internal standard, and the degree of cleavage was calculated from the reduction in the normalized area of the substrate peaks. For the identification of PrtA cleavage site in the fluorescence-quenched substrate, Dabcyl–EVYAVES–Edans, chromatographic peaks of the hydrolysis products were collected, lyophilized and resuspended in 0.1% trifluoroacetic acid. ESI-MS analysis was performed as above.

Use of the Dabcyl–EVYAVES–Edans substrate: determination of the excitation and emission wavelengths, the change in molar fluorescence and correction of the inner filter effect

An excitation scan between 250 and 450 nm (at 475 nm emission wavelength) showed a maximum at 340 nm, whereas comparison of the emission scans (at 340 nm excitation wavelength) of the intact and the completely hydrolysed substrate (after 120 min incubation with PrtA in the darkness) between 360 and 550 nm showed a maximal difference at 495 nm. Therefore, fluorescence intensities were read at 340 nm excitation and 495 nm emission wavelengths.

To calculate the change in molar fluorescence, fluorescence intensities of 0.5, 1.0, 2.0, 4.9, 11.7, 21.2 and 48.5 μM substrate solutions were measured before and after complete hydrolysis by PrtA (in the darkness) in the buffer solution used for activity measurements (see below). Fluorescence values were corrected for the inner filter effect (see below) and plotted as a function of substrate concentration. The difference between the slopes of the curves for the intact and hydrolysed substrate gave the molar fluorescence change, 5.67×10^{11} cps·M^{-1}.

Because of the presence of both an effective absorbant (the quencher) and a fluorophore in the solution, there is a departure from linearity in the fluoresence intensity versus concentration curves. To take into consideration the influence of this inner filter effect, the fluorescence (F) values were corrected using the equation by Puchalski *et al.* [36]:

$$\frac{F_{corrected}}{F_{observed}} = \frac{2.3 \times d \times A_{ex}}{1 - 10^{-d \times A_{ex}}} \times 10^{g \times A_{em}} \times \frac{2.3 \times s \times A_{em}}{1 - 10^{-s \times A_{em}}}$$

where d is the path length of the excitation light in the solution, s is the width of the excitation beam, g is the distance between the edge of the exciting beam and the cuvette wall (1.00, 0.1 and 0.15 cm, respectively, in our measurements), and A_{ex} and A_{em} are the absorbance of the sample solution at the excitation and the emission wavelengths.

Mesurement of PrtA activity and specificity of the Dabcyl–EVYAVES–Edans substrate

Activity measurements were carried out at 30 °C in a 50 mM Tris/HCl (pH 8.0) buffer, containing 10 mM $CaCl_2$, 100 mM NaCl and 0.05 mg·mL^{-1} BSA (assay buffer). Reactions were started by addition of the enzyme, except for the experiments with inhibitors (see below). The reactions were followed in a SPEX Fluoromax^{TM} spectrofluorimeter (SPEX Industries Inc., Edison, NJ), using 340 nm excitation and 495 nm emission wavelengths (see above).

The kinetic parameters of PrtA were determined with saturation kinetics at 1.0 nM enzyme, and 0.5, 1.0, 2.0, 4.9, 11.75, 21.2 and 48.5 μM substrate concentrations with duplicate measurements. Fluorescence versus time curves were recalculated to correct for the inner filter effect (above). To obtain the initial reaction velocities the slope of that part of the corrected curve was used where < 5% of the substrate was consumed (where they were essentially linear). The kinetic constants, K_m and k_{cat}, were calculated from the initial rate versus substrate concentration curves using ENZFITTER 1.05 software (Elsevier-Biosoft, Cambridge, UK).

When the effect of inhibitors and the pH was investigated 0.2 and 0.4 nM PrtA concentrations were used, respectively; the substrate concentration was 1.0 μM in both cases, well below the K_m value, allowing the specificity constants (k_{cat}/K_m) to be calculated directly from the corrected initial reaction rates (see above). The inhibitors, EDTA, phenylmethanesulfonyl fluoride, 1,4-dithiothreitol, and Cys (1.0 mM each) were added to PrtA in 0.7 mL assay buffer (above). After 20-min incubation at room temperature, the remaining activity was determined by starting measurement with the addition of the substrate. The pH-dependence of the PrtA activity was measured in 10 mM $CaCl_2$, 100 mM NaCl and 0.05 mg·mL^{-1} BSA containing solutions, in the presence of 50 mM of the following buffers: sodium acetate (pH 4.5, 5.0, 5.5), Mes/HCl (pH 6.0, 6.5), Mops/HCl (pH 7.0, 7.5), Hepes/HCl (pH 8.0), Tris/HCl (pH 8.5, 9.0) and Caps/HCl (pH 10.0).

The activity of proteases, other than PrtA (OpdA, Php-C, *Clostridium* collagenase, trypsin and chymotrypsin) was measured at 1.0 μM substrate and 2.0–50 nM protease concentration, and the specificity constants (k_{cat}/K_m) were obtained from the corrected initial reaction rates (see above).

Measurements of PrtA activity in insect haemolymph and body homogenate

PrtA activity was measured at 1 or 20 μM Dabcyl–EVYAVES–Edans substrate concentration in the assay

buffer, in 700 μL final volume, at 30 °C starting the reaction by the addition of 10–20 μL *G. mellonella* haemolymph or body homogenate samples (see above). The specificity constants (k_{cat}/K_m) obtained from the corrected initial reaction rates were calculated for 1 μL undiluted haemolymph and body homogenate.

Acknowledgements

This work was supported by research grants T037907 to IV and TS049812 to LG from National Research Foundation (OTKA), Hungary.

References

1 Marokházi J, Lengyel K, Pekár S, Felföldi G, Patthy A, Gráf L, Fodor A & Venekei I (2004) Comparison of proteolytic activities produced by entomopathogenic *Photorhabdus* bacteria: strain- and phase-dependent heterogeneity in composition and activity of four enzymes. *Appl Environ Microbiol* **70**, 7311–7320.

2 Bowen DJ, Rocheleau TA, Grutzmacher CK, Meslet L, Valens M, Marble D, Dowling A, ffrench-Constant R & Blight MA (2003) Genetic and biochemical characterization of PrtA, an RTX-like metalloprotease from *Photorhabdus*. *Microbiology* **149**, 1581–1591.

3 Duchaud E, Rusniok C, Frangeul L, Buchrieser C, Givaudan A, Taourit S, Bocs S, Boursaux-Eude C, Chandler M, Charles JF *et al.* (2003) The genome sequence of the entomopathogenic bacterium *Photorhabdus luminescens*. *Nat Biotechnol* **21**, 1307–1313.

4 Molla A, Matsumoto K, Oyamada I, Katsuki T & Maeda H (1986) Degradation of protease inhibitors, immunoglobulins, and other serum proteins by *Serratia* protease and its toxicity to fibroblast in culture. *Infect Immun* **53**, 522–529.

5 Molla A, Tanase S, Hong YM & Maeda H (1988) Interdomain cleavage of plasma fibronectin by zinc-metalloproteinase from *Serratia marcescens*. *Biochim Biophys Acta* **955**, 77–85.

6 Oda T, Kojima Y, Akaike T, Ijiri S, Molla A & Maeda H (1990) Inactivation of chemotactic activity of C5a by the serratial 56-kilodalton protease. *Infect Immun* **58**, 1269–1272.

7 Tanaka H, Yamamoto T, Shibuya Y, Nishino N, Tanase S, Miyauchi Y & Kambara T (1992) Activation of human plasma prekallikrein by *Pseudomonas aeruginosa* elastase. II. Kinetic analysis and identification of scissile bond of prekallikrein in the activation. *Biochim Biophys Acta* **1138**, 243–250.

8 Belas R, Manos J & Suvanasuthi R (2004) *Proteus mirabilis* ZapA metalloprotease degrades a broad spectrum of substrates, including antimicrobial peptides. *Infect Immun* **72**, 5159–5167.

9 Senior BW, Albrechtsen M & Kerr MA (1987) *Proteus mirabilis* strains of diverse type have IgA protease activity. *J Med Microbiol* **24**, 175–180.

10 Senior BW, Albrechtsen M & Kerr MA (1988) A survey of IgA protease production among clinical isolates of *Proteeae*. *J Med Microbiol* **25**, 27–31.

11 Maeda H & Morihara K (1995) Serralysin and related bacterial proteinases. *Methods Enzymol* **248**, 395–413.

12 Louis D, Bernillon J & Wallach JM (1998) Specificity of *Pseudomonas aeruginosa* serralysin revisited, using biologically active peptides as substrates. *Biochim Biophys Acta* **1387**, 378–386.

13 Louis D, Bernillon J & Wallach JM (1999) Use of a 49-peptide library for a qualitative and quantitative determination of pseudomonal serralysin specificity. *Int J Biochem Cell Biol* **31**, 1435–1441.

14 Fernandes BL, Anéas MA, Juliano L, Palma MS, Lebrun I & Portaro FC (2000) Development of an operational substrate for ZapA, a metalloprotease secreted by the bacterium *Proteus mirabilis*. *Braz J Med Biol Res* **33**, 765–770.

15 Morihara K, Tsuzuki H & Oka T (1973) On the specificity of *Pseudomonas aeruginosa* alkaline proteinase with synthetic peptides. *Biochim Biophys Acta* **309**, 414–429.

16 Schechter I & Berger A (1967) On the size of the active site in proteases. I. Papain. *Biochem Biophys Res Commun* **27**, 157–162.

17 Anéas MA, Portaro FC, Lebrun I, Juliano L, Palma MS & Fernandes BL (2001) ZapA, a possible virulence factor from *Proteus mirabilis* exhibits broad protease substrate specificity. *Braz J Med Biol Res* **34**, 1397–1403.

18 Baumann U, Wu S, Flaherty KM & McKay DB (1993) Three-dimensional structure of the alkaline protease of *Pseudomonas aeruginosa*: a two-domain protein with a calcium binding parallel beta roll motif. *EMBO J* **12**, 3357–3364.

19 Stöcker W, Grams F, Baumann U, Reinemer P, Gomis-Rüth FX, McKay DB & Bode W (1995) The metzincins – topological and sequential relations between the astacins, adamalysins, serralysins, and matrixins (collagenases) define a superfamily of zinc-peptidases. *Protein Sci* **4**, 823–840.

20 Baumann U, Bauer M, Létoffe S, Delepelaire P & Wandersman C (1995) Crystal structure of a complex between *Serratia marcescens* metallo-protease and an inhibitor from *Erwinia chrysanthemi*. *J Mol Biol* **248**, 653–661.

21 Hege T & Baumann U (2001) Protease C of *Erwinia chrysanthemi*: the crystal structure and role of amino acids Y228 and E189. *J Mol Biol* **314**, 187–193.

22 Bae KH, Kim IC, Kim KS, Shin YC & Byun SM (1998) The Leu-3 residue of *Serratia marcescens* metalloprotease inhibitor is important in inhibitory activity

and binding with *Serratia marcescens* metalloprotease. *Arch Biochem Biophys* **352**, 37–43.
23 Duong F, Lazdunski A, Cami B & Murgier M (1992) Sequence of a cluster of genes controlling synthesis and secretion of alkaline protease in *Pseudomonas aeruginosa*: relationships to other secretory pathways. *Gene* **121**, 47–54.
24 Valens M, Broutelle AC, Lefebvre M & Blight MA (2002) A zinc metalloprotease inhibitor, Inh, from the insect pathogen *Photorhabdus luminescens*. *Microbiology* **148**, 2427–2437.
25 Hege T, Feltzer RE, Gray RD & Baumann U (2001) Crystal structure of a complex between *Pseudomonas aeruginosa* alkaline protease and its cognate inhibitor: inhibition by a zinc–NH_2 coordinative bond. *J Biol Chem* **276**, 35087–35092.
26 Bond MD & Van Wart HE (1984) Characterization of the individual collagenases from *Clostridium histolyticum*. *Biochemistry* **23**, 3085–3091.
27 Beekman B, van El B, Drijfhout JW, Ronday HK & TeKoppele JM (1997) Highly increased levels of active stromelysin in rheumatoid synovial fluid determined by a selective fluorogenic assay. *FEBS Lett* **418**, 305–309.
28 Marokházi J, Kóczán G, Hudecz F, Gráf L, Fodor A & Venekei I (2004) Enzymic characterization with progress curve analysis of a collagen peptidase from an enthomopathogenic bacterium, *Photorhabdus luminescens*. *Biochem J* **379**, 633–640.
29 Sigman JA, Edwards SR, Pabon A, Glucksman MJ & Wolfson AJ (2003) pH dependence studies provide insight into the structure and mechanism of thimet oligopeptidase (EC 3.4.24.15). *FEBS Lett* **545**, 224–228.
30 Bowen D, Blackburn M, Rocheleau T, Grutzmacher C & ffrench-Constant RH (2000) Secreted proteases from *Photorhabdus luminescens*: separation of the extracellular proteases from the insecticidal Tc toxin complexes. *Insect Biochem Mol Biol* **30**, 69–74.
31 Schmidt TM, Bleakley BH & Nealson KH (1988) Characterization of an extracellular protease from the insect pathogen *Xenorhabdus luminescens*. *Appl Environ Microbiol* **54**, 2793–2797.
32 Gomis-Rüth FX, Maskos K, Betz M, Bergner A, Huber R, Suzuki K, Yoshida N, Nagase H, Brew K, Bourenkov GP *et al*. (1997) Mechanism of inhibition of the human matrix metalloproteinase stromelysin-1 by TIMP-1. *Nature* **389**, 77–81.
33 Mock WL & Yao J (1997) Kinetic characterization of the serralysins: a divergent catalytic mechanism pertaining to astacin-type metalloproteases. *Biochemistry* **36**, 4949–4958.
34 Daborn PJ, Waterfield N, Blight MA & ffrench-Constant RH (2001) Measuring virulence factor expression by the pathogenic bacterium *Photorhabdus luminescens* culture and during insect infection. *J Bacteriol* **183**, 5834–5839.
35 ffrench-Constant R, Waterfield N, Daborn P, Joyce S, Bennett H, Au C, Dowling A, Boundy S, Reynolds S & Clarke D (2003) *Photorhabdus*: towards a functional genomic analysis of a symbiont and pathogen. *FEMS Microbiol Rev* **26**, 433–456.
36 Puchalski MM, Morra MJ & von Wandruszka R (1990) Assessment of inner filter effect corrections in fluorimerty. *Fr J Anal Chem* **340**, 341–344.